ELSEVIER

Journal of Crystal Growth 244 (2002) 318–326

JOURNAL OF CRYSTAL GROWTH

www.elsevier.com/locate/jcrysgro

Growth mechanism and electrical properties of $Pb[(Zn_{1/3}Nb_{2/3})_{0.91}Ti_{0.09}]O_3$ single crystals by a modified Bridgman method

Bi-Jun Fang*, Hai-Qing Xu, Tian-Hou He, Hao-Su Luo, Zhi-Wen Yin

The State Key Laboratory of High Performance Ceramics and Superfine Microstructure, Shanghai Institute of Ceramics, Chinese Academy of Sciences, 201800 Shanghai, China

Communicated by D.P. Norton

Abstract

Relaxor-based piezoelectric $Pb[(Zn_{1/3}Nb_{2/3})_{0.91}Ti_{0.09}]O_3$ (PZNT 91/9) single crystals 28 mm in diameter and 30 mm in length were grown by a modified Bridgman technique with PbO flux using an allomeric seed crystal. The crystals were grown in sealed platinum crucibles at about 1250°C. The obtained crystals are of pure perovskite structure within the sensitivity of X-ray diffraction measurement and the as-grown crystals have three appearing faces with slight deviation in angle from the pseudocubic $(0\,0\,1)_{cub}$ face. The growth mechanism of the PZNT crystals could be explained from the viewpoint of the formation of growth units and the incorporation of growth units into different interfaces of the crystal lattice. The growth rate of various crystal faces is related to the assembling modes of the growth units into different interfaces. Assembling of $[BO_6]$ octahedral growth unit into $(1\,1\,1)_{cub}$ interface has the strongest bonding force, and this crystal direction has the fastest growth rate; therefore, $(1\,1\,1)_{cub}$ crystal face disappears, assembling of $[BO_6]$ into $(0\,0\,1)_{cub}$ interface has the smallest bonding force, and this crystal face has the smallest growth rate; therefore, $(0\,0\,1)_{cub}$ crystal face appears. The growth steps aligning approximately along the $\langle 0\,0\,1\rangle_{cub}$ direction reveal that $(0\,0\,1)_{cub}$ face proceeds by a layer growth mechanism controlled by two-dimensional nucleation starting at crystal corners or edges. Dielectric measurement proves that the quality of the obtained PZNT crystals is good. Domain observation shows that both the rhombohedral and tetragonal orientation state domain coexist in the morphotropic PZNT 91/9 single crystals.

PACS: 81.10; 61.72.J; 78.20.C

Keywords: A1. Growth models; A2. Bridgman technique; A2. Growth from solutions; B1. Perovskites; B2. Ferroelectric materials; B2. Piezoelectric materials

1. Introduction

Relaxor ferroelectric $Pb(Zn_{1/3}Nb_{2/3})O_3$ (PZN) is characterized by a diffuse maximum of dielectric constant associated with a strong frequency dispersion. The relaxor properties can be attributed to the

*Corresponding author.
E-mail address: fangbj@sohu.com (B.-J. Fang).

0022-0248/02/$ - see front matter
PII: S0022-0248(02)01662-7

self-assembled ordered/disordered nanostructures and the formation of local polar domains [1]. On the other hand, $PbTiO_3$ (PT) shows typical long-range ferroelectric (FE) properties with ferroelectric–paraelectric (PE) phase transition at $T_C = 490°C$. Substitution of Ti^{4+} ions for the complex $(Zn_{1/3}Nb_{2/3})^{4+}$ ions on the B-site will result in the formation of long-range ferroelectric phases. Therefore, the solid solutions of $(1-x)Pb(Zn_{1/3}Nb_{2/3})O_3$–$xPbTiO_3$ ($(1-x)$PZN–xPT) are expected to combine the advantages of both relaxor ferroelectric PZN and ferroelectric PT. Indeed, single crystals of PZNT were reported to exhibit an extremely large piezoelectric constant ($d_{33} > 2000$ pC/N), piezoelectric strain ($> 1\%$) and a very high electromechanical coupling factor ($k_{33} > 90\%$) [2,3]. Such excellent performance has triggered much attention on the research of this material, and it also makes PZNT crystals a much better candidate for transducer materials than the $PbZrO_3$–$PbTiO_3$ (PZT) system in a broad range of advanced applications [4].

From the viewpoint of crystal chemistry, the outstanding properties of the relaxor-based piezocrystals are closely related to the morphotropic phase boundary (MPB) effects and the formation of macro-domain states resulting from the substitution of Ti^{4+} ions for the complex ions $(Zn_{1/3}Nb_{2/3})^{4+}$ on the B-site of perovskite structure [5]. The MPB for the $(1-x)$PZN–xPT system is located at $x \approx 0.08-0.105$, which separates a rhombohedral from a tetragonal phase [6]. Compared to the growth of PZT single crystals, PZNT crystals are relatively easily grown from flux over the wide solid solution range $0 \leqslant x \leqslant 0.2$ [2]. Of all the solid solutions, $Pb[(Zn_{1/3}Nb_{2/3})_{0.91}Ti_{0.09}]O_3$ (PZNT 91/9) with the composition near MPB is of great interest because of its excellent performance. Kobayashi et al. have reported large PZNT 91/9 single crystals (the largest obtained single crystal with the size of $43 \times 42 \times 40\,mm^3$) fabricated by a conventional flux method [7]. However, flux method is unsuitable for growing large PZNT crystals because it is difficult to control spontaneous nucleation during crystal growth. In contrast, Bridgman process allows for the manufacture of crystals with controlled dimension and good reproducibility. Yamashita et al. have confirmed that flux Bridgman method is suitable for mass-producing large PZNT 91/9 crystals for practical applications [8,9].

In this work, we developed a novel modified Bridgman technique to grow PZNT 91/9 single crystals with an allomeric seed crystal. From crystal morphology we put forward a growth mechanism for the growth of PZNT crystals from PbO flux. The chemical and physical properties of the PZNT crystals were characterized by X-ray diffraction and dielectric measurement.

2. Crystal experiments and results

PZNT single crystals were grown by a modified Bridgman method. High purity (more than 99.9%) agent powders of PbO, ZnO, Nb_2O_5 and TiO_2 were dried before weighing. The mixture of these powders was maintained in the ratios of PZN:PT = 91:9 and PZNT:PbO = 45:55 in mole percentage. PbO acted as flux. The raw materials were precalcined by B-site precursor synthesis method, which can prevent, to some extent, the formation of pyrochlore phase [10,11]. PZNT crystals were grown in sealed platinum crucibles to prevent the evaporation of PbO during crystal growth.

PZNT crystals were grown at about 1250°C, which was higher than that of the supported Bridgman method used by Yamashita et al. [9]. Other conditions included a temperature gradient of about 30–50°C/cm at the solid–liquid interface, allomeric $Pb[(Mg_{1/3}Nb_{2/3})_{0.69}Ti_{0.31}]O_3$ (PMNT 69/31) seed crystals along $\langle 1\,1\,1 \rangle_{cub}$ direction and $MoSi_2$ resistance heater elements. After soaking for 6 hrs in the center of the furnace, the crucibles with their charges were pulled down at the rate of 0.2–0.6 mm/h [12].

It was possible to obtain four PZNT91/9 crystal boules simultaneously by this method. Temperature gradient is an important consideration for Bridgman technique. Fig. 1 shows the temperature gradient of the Bridgman furnace. The temperature gradient could be dominated at around 30–50°C/cm at the solid–liquid interface by this method, which was ideal for the crystal growth.

PZNT91/9 single crystals 28 mm in diameter and 30 mm in length were obtained. The as-grown crystals exhibit dark-brown color on their surface due to a thin coat of PbO flux. After flux removal by boiling

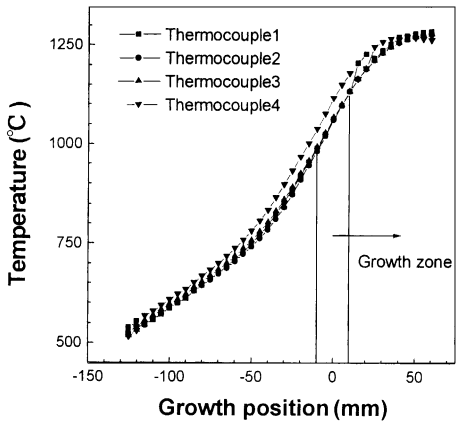

Fig. 1. Axial temperature gradient profile of the Bridgman furnace for the growth of PZNT 91/9 single crystals.

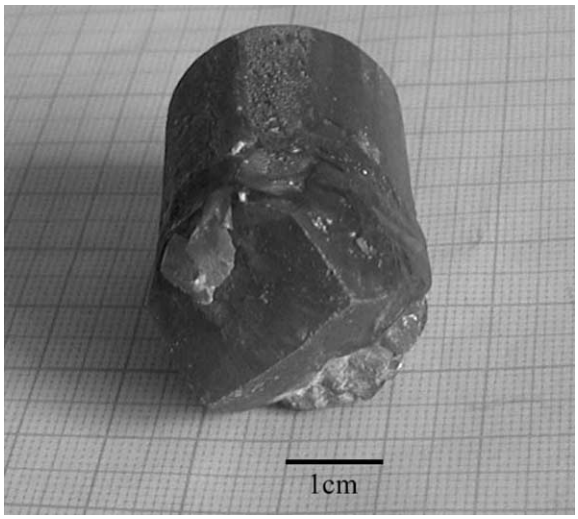

Fig. 2. Morphology of appearing faces of a PZNT 91/9 single crystal grown by a flux Bridgman method.

acetic acid, the obtained crystals show three appearing faces which deviate slightly in angle from the pseudocubic $(0\,0\,1)_{cub}$ face as determined by Laue X-ray diffraction technique. The inclinations between the three appearing faces are about 97°. Due to the deviation from the $\langle 1\,1\,1\rangle_{cub}$ direction of the PMNT 69/31 seed crystal and variation of growth conditions, the development extent of the three appearing faces is different. Fig. 2 shows the morphology of the appearing faces of an as-grown PZNT crystal from which we can see how an appearing face extremely degenerates.

3. X-ray diffraction analysis

B-site precursor synthesis of raw materials can effectively reduce the formation of pyrochlore phase during crystal growth. Fig. 3 shows the X-ray diffraction patterns of the precalcined and postcalcined

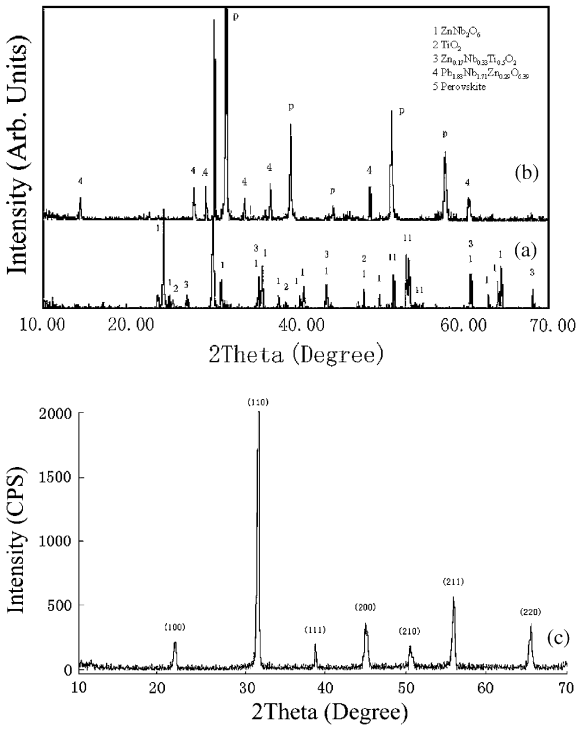

Fig. 3. X-ray diffraction patterns of presynthesized raw materials by B-site precursor synthesis method: (a) powder of ZnO, Nb_2O_5 and TiO_2 precalcined at 950°C; (b) resulting powder of (a) with the addition of stoichiometric PbO postcalcined at 750°C and of the obtained PZNT 91/9 single crystal (c).

powders by B-site precursor synthesis method (Rigaku D/MAX-3C X-ray diffractometer). The lattice structure of the obtained PZNT crystals is also shown in Fig. 3, from which we can see after being precalcined the main phase of the resultant powder is $ZnNb_2O_6$ with columbite structure. After the addition of stoichiometric PbO, the main phase of the postcalcined powder is already $Pb[(Zn_{1/3}Nb_{2/3})_{0.91}Ti_{0.09}]O_3$ with perovskite structure. There is still a little pyrochlore phase, which is $Pb_{1.83}Nb_{1.71}Zn_{0.29}O_{6.39}$-type, but the content is small. During crystal growth, the remaining pyrochlore phase could change into perovskite structure. Fig. 3(c) shows that the obtained PZNT crystals are of pure perovskite structure within the sensitivity of X-ray diffraction.

Based on the results discussed above, the process of the formation of perovskite PZNT 91/9 crystal from PbO flux environment could be delineated as follows**:**

Presynthesized stage:

$$0.303ZnO + 0.303Nb_2O_5 + 0.09TiO_2 \rightarrow 0.303(1-x)ZnNb_2O_6 + 1.811xZn_{0.17}Nb_{0.33}Ti_{0.5}O_2 + (0.09 - 0.906x)TiO_2(\text{trace}), \quad (1)$$

$$0.303(1-x)ZnNb_2O_6 + 1.811xZn_{0.17}Nb_{0.33}Ti_{0.5}O_2 + (0.09 - 0.906x)TiO_2(\text{trace}) + PbO \rightarrow (1-1.83y)Pb[(Zn_{1/3}Nb_{2/3})_{0.91}Ti_{0.09}]O_3 + yPb_{1.83}Nb_{1.71}Zn_{0.29}O_{6.39} + 0.265yZnO - 0.2999yNb_2O_5 + 0.165yTiO_2. \quad (2)$$

Crystal growth stage:

$$(1-1.83y)\mathrm{Pb}[(\mathrm{Zn}_{1/3}\mathrm{Nb}_{2/3})_{0.91}\mathrm{Ti}_{0.09}]\mathrm{O}_3 + y\mathrm{Pb}_{1.83}\mathrm{Nb}_{1.71}\mathrm{Zn}_{0.29}\mathrm{O}_{6.39} + 0.265y\mathrm{ZnO} - 0.2999y\mathrm{Nb}_2\mathrm{O}_5 + 0.165y\mathrm{TiO}_2 \xrightarrow{\text{PbO flux environment}} 1.0\mathrm{Pb}[(\mathrm{Zn}_{1/3}\mathrm{Nb}_{2/3})_{0.91}\mathrm{Ti}_{0.09}]\mathrm{O}_3(\text{perovskite}). \quad (3)$$

These reaction schemes justify all the necessary requirements of mass balance and explain the results of XRD patterns.

4. Crystal growth mechanism

The obtained PZNT crystals always have three appearing faces (Fig. 2). Laue X-ray diffraction determines that the appearing faces are pseudocubic $(0\,0\,1)_{\mathrm{cub}}$ face with a slight deviation in angle. Smoothly developed $(0\,0\,1)_{\mathrm{cub}}$ faces indicate that the mean $\langle 0\,0\,1\rangle_{\mathrm{cub}}$ direction was of the far slower growth direction according to the theory of crystal growth.

Crystal growth is mainly determined by the internal structure of a given crystal, and affected by external conditions. The periodic bond chain theory (PBC theory) is the mainly theoretical model concerning crystal growth. In general, the growth morphology of a crystal is determined by the relative growth rates of all possible faces. The lower the growth rate one face has, the bigger its morphological importance will be. Therefore, the growth morphology of a crystal should be exclusively composed of the so-called flat faces (F faces), those which contain at least two non-parallel PBCs. PBC is defined as an uninterrupted sequence of periodically repeated strong bonds in a certain crystallographic direction, and the PBC theory provides an ideal growth habit of crystals in terms of bond chain types between molecules and attachment energy. However, this model has some shortage in explaining crystal growth habit of polar crystals. Wei-Zhuo Zhong put forward the growth unit model, which hypothesizes that in the crystallization procedure, crystal structure was composed of negative ion coordination polyhedrons whose couplings are positive ions, and the coordination polyhedron possessing crystal structure is called a growth unit [13].

During crystal growth, PZNT crystals are in cubic PE structure with space group Pm3 m. The location of structural ions is

$\mathrm{Pb}^{2+}(0,0,0)$,

$\mathrm{Nb}^{5+}, \mathrm{Zn}^{2+}, \mathrm{Ti}^{4+}(\frac{1}{2},\frac{1}{2},\frac{1}{2})$(ordered or disordered),

$3\mathrm{O}^{2-}(\frac{1}{2},\frac{1}{2},0)$; $(\frac{1}{2},0,\frac{1}{2})$; $(0,\frac{1}{2},\frac{1}{2})$.

From a kinetics viewpoint of crystal growth it is assumed that the growth mechanism mainly contains the formation of growth units and the incorporation of growth units into the crystal lattice at the interface. The problem is to clarify what the growth units are for a given location and then how growth units are incorporated into the crystal lattice. PZNT is ionic crystal; the bonds of A–O and B–O in this structure are all ionic. X-ray pattern of $\mathrm{Pb}[(\mathrm{Mg}_{1/3}\mathrm{Nb}_{2/3})_{0.76}\mathrm{Ti}_{0.24}]\mathrm{O}_3$ (PMNT 76/24) melt quenched from high temperature shows that the melt is similar in structure with the crystal. This indicates the possibility of existence of growth units based on $[\mathrm{MgO}_6]^{10-}$, $[\mathrm{NbO}_6]^{7-}$ and $[\mathrm{TiO}_6]^{8-}$ negative ion coordination octahedrons [14]. Therefore, there may also be $[\mathrm{ZnO}_6]^{10-}$, $[\mathrm{NbO}_6]^{7-}$ and $[\mathrm{TiO}_6]^{8-}$ growth units in PZNT melt. So we introduce the hypothesis that the growth units are the complexes formed by the attraction of cations and O^{2-} ions, whose coordination numbers are equal to that of the cations in the crystal to be formed. From the calculation value of the stability energy of the coordination octahedrons, $[\mathrm{ZnO}_6]^{10-}$, $[\mathrm{NbO}_6]^{7-}$ and $[\mathrm{TiO}_6]^{8-}$ are advantageous growth units [14,15]. Fig. 4 shows the schematic diagram of connecting of coordination octahedron growth units by Pb^{2+} ions in PZNT crystal.

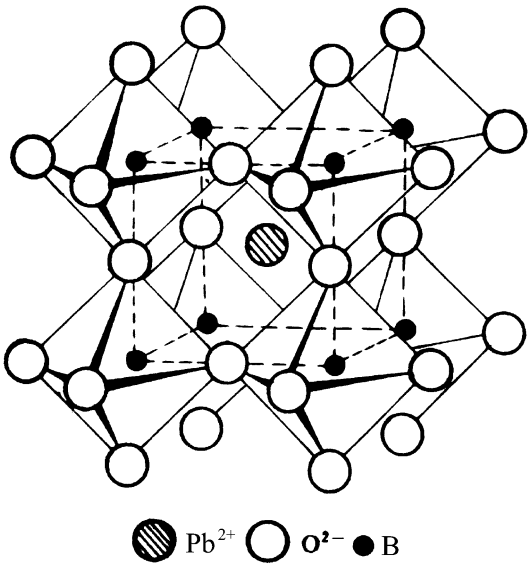

Fig. 4. Schematic diagram of perovskite structure ABO_3 composed of $[BO_6]$ octahedral growth units and Pb^{2+} ions.

The growth mechanism of the PZNT crystal can be considered as the stacking order of the coordination octahedrons by sharing elements (corner, edge or face of the coordination octahedrons). In the interior of the crystal, coordination octahedrons are connected by sharing Pb^{2+} ions, while at the interface of the crystal, the terminal vertex of elements (corner, edge or face) of the coordination octahedrons couple with O^{2-} ions. Considering the assembling of $[BO_6]$ growth unit at the $\{0\,0\,1\}_{cub}$, $\{1\,1\,0\}_{cub}$ and $\{1\,1\,1\}_{cub}$ growth interface during crystal growth, although $[BO_6]$ octahedron incorporated into the three interfaces with terminal vertex, the assembling of these growth units at different interfaces is different. This determines the stability difference of the assembling of growth units at different interface as well as leads the anisotropic growth rate of various crystal faces.

In PZNT crystal, when $[BO_6]$ octahedron incorporates into $(0\,0\,1)_{cub}$ interface, it just bonds with one growth unit of $(0\,0\,1)_{cub}$ face using one terminal vertex. The stability of this assembling mode is poor. Therefore, only formation of two-dimensional crystal nucleation can start crystal growth at crystal corners or edges. Detailed surface micro-morphology observation has revealed the growth steps aligning approximately along $\langle 0\,0\,1\rangle_{cub}$ direction, indicating a dominant layer growth mechanism for the $\{0\,0\,1\}_{cub}$ face (Fig. 5).

When $[BO_6]$ octahedron assembles into kinked $(1\,1\,1)_{cub}$ interface, it could bond with three vertexes of growth units in $(1\,1\,1)_{cub}$ interface using three terminal vertexes. Fig. 6 shows the diagram of $[BO_6]$ octahedron growth unit incorporating into $(1\,1\,1)_{cub}$ face. When octahedrons assemble in this mode, the number of formation of chemical bond is many. Therefore, the terminal vertexes of the coordination octahedron have the strongest bonding force in this direction. Crystal growth along this direction has no need of the process of nucleation, and the growth rate is fast. Similarly, when $[BO_6]$ octahedral growth unit incorporates into $(1\,1\,0)_{cub}$ interface, the stability of this assembling mode will be in between the above two assembling modes.

According to the above analysis we can judge the growth habit using the assembling mode of the coordination octahedrons incorporating different interfaces. Namely, the assembling of coordination octahedrons at different interfaces is different, and the growth rate of various crystal faces is related to the assembling modes of the growth units into different interfaces. Assembling of $[BO_6]$ octahedral growth

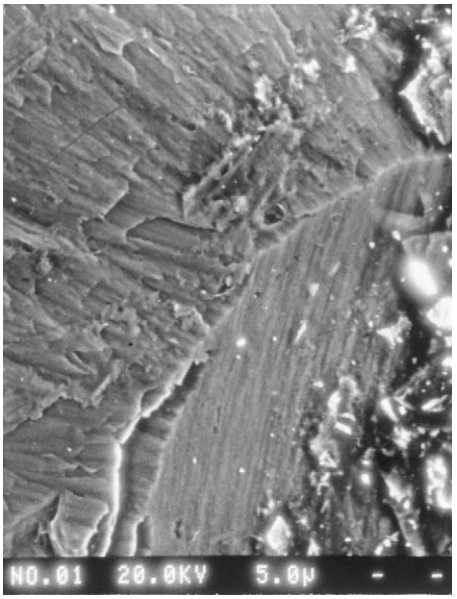

Fig. 5. Surface micro-morphology of an appearing face of a PZNT 91/9 crystal showing layered growth steps along $(0\,0\,1)_{cub}$.

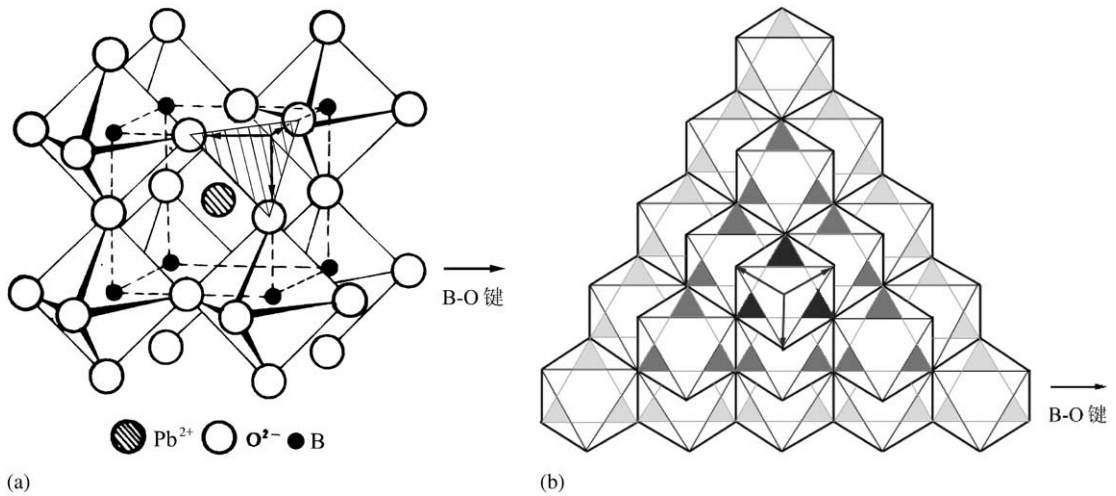

Fig. 6. Assembling of $[BO_6]$ octahedral growth units along the $\langle 1\,1\,1\rangle_{cub}$ direction (the equilateral triangles in the right figure of Fig. 6 denote the coordination complexes formed by the attraction of cations B and O^{2-} ions seen along $\langle 1\,1\,1\rangle_{cub}$ direction, the junction points of the equilateral hexagons denote Pb^{2+} ions).

units into $(1\,1\,1)_{cub}$ interface has the strongest bonding force, and the direction of this crystal face has the fastest growth rate; the assembling of $[BO_6]$ into $(0\,0\,1)_{cub}$ interface has the smallest bonding force, and this crystal face has the smallest growth rate; and assembling of $[BO_6]$ into $(1\,1\,0)_{cub}$ interface has the second strongest bonding force, and this direction has the second faster growth rate. According to the theory of crystal growth, crystal faces whose growth rate is slow easily appear and crystal faces whose growth rate is

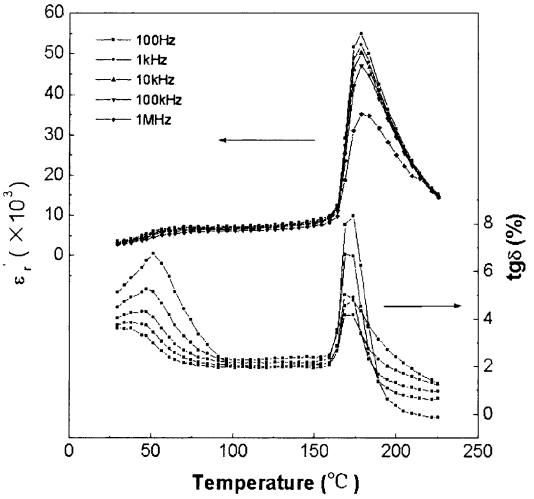

Fig. 7. Temperature and frequency dependence of dielectric constant and dissipation factor of an unpoled (0 0 1) PZNT 91/9 plane crystal.

fast easily disappear; therefore, the $(1\,1\,1)_{cub}$ crystal face of the crystal from flux disappears. The $(0\,0\,1)_{cub}$ crystal face appears, and $(1\,1\,0)_{cub}$ crystal face may appears sometimes, but we have not observed this phenomenon in our experiments.

5. Ferroelectric properties

Dielectric property of the grown PZNT crystals was measured by means of an impedance analyzer (HP4192A). Fig. 7 shows dielectric constant and dissipation factor dependence on temperature at different frequencies of an unpoled (0 0 1) PZNT crystal plate. There are two obvious anomalies at about 61°C and 177°C, corresponding to phase transition from rhombohedral FE phase to tetragonal FE phase and cubic PE phase with increasing temperature. Comparing with typical relaxor ferroelectric behavior, the maximum of dielectric constant and dissipation factor at various frequencies are nearly at the same temperature. This indicates the enhancement of long-range ferroelectric order due to the substitution of Ti^{4+} ions for ions $(Zn_{1/3}Nb_{2/3})^{4+}$ in the PZNT 91/9 crystal. Frequency dispersion appears at around Curie temperature, indicating that the relaxor behavior is retained to some extent. Domain observation confirms that domain structure of the morphotropic PZNT91/9 crystals are composed of a mixture of both the rhombohedral and tetragonal orientation states, as reported in Ref. [16].

6. Conclusions

$Pb[(Zn_{1/3}Nb_{2/3})_{0.91}Ti_{0.09}]O_3$ (PZNT 91/9) single crystals 28 mm in diameter and 30 mm in length were grown by a modified Bridgman method with PbO flux using an allomeric seed crystal. The obtained crystals have three appearing faces which deviate slightly in angle from the pseudocubic $(0\,0\,1)_{cub}$ face. The inclinations between the three appearing faces are about 97°. The growth mechanism of the PZNT crystal could be considered as the stacking order of the coordination octahedral growth units by sharing elements (corner, edge or face of the coordination octahedrons) at different interfaces of the crystal. The growth rate

of various crystal faces is related to the assembling modes of the growth units into different interfaces. Assembling of $[BO_6]$ octahedral growth units into $(1\,1\,1)_{cub}$ interface has the strongest bonding force, and this crystal direction has the fastest growth rate; therefore, $(1\,1\,1)_{cub}$ crystal face disappears, assembling of $[BO_6]$ into $(0\,0\,1)_{cub}$ interface has the smallest bonding force, and this crystal face has the smallest growth rate; therefore, $(0\,0\,1)_{cub}$ crystal face appears. Detailed surface micro-morphology observation reveals that growth steps aligning approximately along $\langle 0\,0\,1\rangle_{cub}$ direction, which indicates that $(0\,0\,1)_{cub}$ face proceeds by a layer growth mechanism controlled by two-dimensional nucleation starting at crystal corners or edges. Dielectric measurement shows that the morphotropic PZNT 91/9 crystals retain the relaxor behavior to some extent. The enhanced dielectric performance has proved the high quality of the obtained PZNT crystals.

Acknowledgements

The authors would like to thank the National Sciences Foundation of China (Grant Nos. 59995520 and 59872048) and the Shanghai Municipal Government (Grant No. 005207015) for the financial support. One of the authors (Dr. Bi-Jun Fang) is thankful to Dr. Gui-Sheng Xu of Shanghai Institute of Ceramics of Chinese Academy of Sciences for helpful suggestions.

References

[1] L.E. Cross, Ferroelectrics 76 (1987) 241.
[2] F. Jiang, S. Kojima, Jpn. J. Appl. Phys. 38 (1999) 5128.
[3] S.-E. Park, T.R. Shrout, J. Mater. Res. Innov. 1 (1997) 20.
[4] S. Saitoh, T. Kobayashi, K. Harada, S. Shimanuki, Y. Yamashita, IEEE Trans. Ultrasonics Ferroelectrics Frequency Control 45 (4) (1998) 1071.
[5] M. Dong, Z.-G. Ye, J. Crystal Growth 209 (2000) 81.
[6] J. Kuwata, K. Uchino, S. Nomura, Jpn. J. Appl. Phys. 21 (9) (1982) 1298.
[7] T. Kobayashi, S. Shimanuki, S. Saitoh, Y. Yamashita, Jpn. J. Appl. Phys. 36 (1997) 6035.
[8] S. Shimanuki, S. Saito, Y. Yamashita, Jpn. J. Appl. Phys. 37 (1998) 3382.
[9] K. Harada, Y. Hosono, S. Saitoh, Y. Yamashita, Jpn. J. Appl. Phys. 39 (2000) 3117.
[10] M. Orita, H. Satoh, K. Aizawa, Jpn. J. Appl. Phys. 31 (1992) 3261.
[11] D.-H. Lee, N.-K. Kim, Mater. Lett. 34 (1998) 299.
[12] H.-S. Luo, G.S. Xu, H.Q. Xu, P.-C. Wang, Z.-W. Yin, Jpn. J. Appl. Phys. 39 (2000) 5581.
[13] W.-Z. Zhong, G.-Z. Liu, Sci. China (B) 24 (4) (1994) 394.
[14] G.-S. Xu, H.-S. Luo, W.-Z. Zhong, Z.-W. Yin, K. Liu, Acta Chim. Sin. 58 (2) (2000) 172.
[15] W.-Z. Zhong, D.-Y. Tang, J. Crystal Growth 166 (1996) 91.
[16] Z.-G. Ye, M. Dong, L. Zhang, Ferroelectrics 229 (1999) 223.